# MAGNETIC STRATIFICATION DURING FLIPPING OF ANTIFERROMAGNETIC MANGANESE FLUORIDE SUBLATTICES

K. L. DUDKO, V. V. EREMENKO, and V. M. FRIDMAN

Physico-technical Low-temperature Institute, Ukrainian Academy of Sciences

Submitted February 12, 1971

Zh. Eksp. Teor. Fiz. 61, 678–688 (August, 1971)

The magnetic properties of the uniaxial antiferromagnetic dielectric $MnF_2$ are studied experimentally in a narrow magnetic field range near $H_0 \approx 92$ kOe. The results show that when the field is deviated from the crystal symmetry axis by an angle not exceeding 30′, the sublattice flipping process is accompanied by the appearance of magnetic stratification in the sample, Certain regions differ both in direction and magnitude of the specific magnetization. This type of domain structure is thermodynamically stable and is analogous to the intermediate state structure in superconductors.

## 1. INTRODUCTION

In a number of substances phase changes occur with a change in magnetic moment:

$$\Delta \mathbf{M} = \mathbf{M}_2 - \mathbf{M}_1,$$

where $\mathbf{M}_1$ and $\mathbf{M}_2$ are the magnetizations of the individual phases. In an infinitely long cylindrical sample this change occurs suddenly at a certain critical value of the longitudinal magnetic field $\mathbf{H}_C$. In bodies of any other shape there should be a domain structure in a finite interval of fields near $\mathbf{H}_C$, i.e., a stratification of the sample into alternating regions of coexisting phases with different values of the magnetic moment $\mathbf{M}_1$ and $\mathbf{M}_2$[1].

Presently domain structure is observed in magnetic substances in which the phase transitions have an entirely different character. In ferromagnets and substances that possess spontaneous magnetization, the change in orientation occurs at $\mathbf{H}_0 = 0$, and the domain strata differ by the direction of the vector $\mathbf{M}$[2]. In other substances magnetic-moment jumps are observed at finite magnitudes of the magnetic field and resemble first-order phase transitions. The domain layers in these cases differ from each other not only in the direction, but also in the absolute magnitude of the magnetization. Such, in fact, is the structure of the intermediate state of superconductors[1].

Not long ago the existence of domain structure was detected[3] and given theoretical explanation[4] in nonferromagnetic metals in which the first-order phase transitions are associated with the de Haas-van Alphen effect. Magnetic stratification similar to the intermediate state of superconductors should also be observed in other substances in which first-order magnetic phase transitions take place.[4]

It would be interesting to try to observe this domain structure in antiferromagnetic dielectrics. In these the phase transitions are associated with readjustment of the magnetic structure under the action of a strong magnetic field.[5] In particular, the phenomenon of flipping of the sublattices of a uniaxial two-sublattice antiferromagnet is well known.[5-8] The periodic domain structure formed in this phase transition was considered theoretically by Bar'yakhtar, Borovik, and Popov.[9] The nucleation and characteristics of the domain walls have been discussed.[10] However, the existing experimental data on magnetic phase transitions in antiferromagnets can be interpreted without assuming magnetic stratification, although they do not contradict this hypothesis.

In this paper we investigate the uniaxial antiferromagnet $MnF_2$ ($T_N = 67$ K), the comparatively simple properties of which are explained by a low spin-orbit interaction energy. Sublattice flipping was observed, and its general features investigated by Jacobs.[11] The magnitude of the critical field for $MnF_2$ is 92 kOe, and the change in magnetic moment is $\Delta M \approx \chi_\perp H_C = 98$ cgs emu. The magnetic properties in the immediate vicinity of the critical field have not been investigated.

A quantity that is sensitive to the formation of domain structure is the magnetic susceptibility. Its dependence on the sample shape is universal for domain structures in different substances[1] and has been used for indirect confirmation of the existence of magnetic layering in beryllium.[3]

Besides measurements of the magnetic susceptibility we used another method to demonstrate the existence of magnetic stratification, namely, the specifics of the magnetic transition itself. That is, when the sublattices flip there arises not only a longitudinal, but also a transverse component of the magnetization $M_\perp$[7,8], which passes through a definite maximum value $M_{\perp 0}$ at $H_0 \approx H_C$. If the process of sublattice flipping proceeds inhomogeneously over the sample volume, the average value of $M_{\perp 0}$ will turn out to be too low, and we therefore have unequivocal information about the presence of magnetic stratification in the critical field region.

Theory indicates that the existence of the magnetic phase transition is limited to a narrow region of angles $\psi < \psi_C$ between the direction of the applied field and the crystal symmetry axis.[7,8] The magnitude of the critical angle $\psi_C$ is determined from the ratio of the anisotropy energy to the exchange energy and is about 0.4° for $MnF_2$.[12] Beyond these limits the sublattices rotate smoothly at $H_0 \approx 92$ kOe, and their is no domain structure. This circumstance makes it easy to distinguish the properties associated with the presence of

domains by a small change in the angle $\psi$.

We describe below our experimental study of the magnetic properties of $MnF_2$ in the vicinity of the critical field. The results cannot be explained without assuming that magnetic stratification exists.

## 2. MEASUREMENT METHOD AND SAMPLES

This problem places extremely stringent requirements on the magnetic measurements. The low transition temperature for $MnF_2$ means that the sample must be cooled to the boiling temperature of liquid helium, and the high critical field requires pulsed magnetic fields. The phenomenon is observed over a narrow range of field intensities $\Delta H$, and its study requires high homogeneity of the magnetic field in the sample, comparable to the conditions for the high-frequency de Haas-van Alphen effect in metals. Thorough investigation of the properties in a narrow region requires the inclusion of a registering apparatus for attaining strictly definite values of the pulsed magnetic field (accuracy of 0.1% or so). The domain structure is expected to appear in a narrow range of $\psi$ (about 0.4°); hence the direction of the field with respect to the crystal symmetry axis must be controlled with a precision of a minute of arc or two. Finally, the nature of the transition requires us to look for changes in not just one component of the magnetization vector, as usual, but in all three simultaneously.

The induction method was used.[11] The samples were cooled by liquid helium in a cryostat finger inside a solenoid. The multiturn pulse solenoid, cooled by liquid nitrogen, had a ratio of length (100 mm) to internal diameter (20 mm), that guaranteed a uniform field over the sample. The homogeneity critierion was the degree of sharpness of the effect itself. To produce the magnetic field pulse, a battery of high-voltage capacitors was discharged through the solenoid. The sample was first oriented so that its fourfold axis of symmetry, determined by x-rays to within ±2°, was along the magnetic field. The cryostat construction provides free access to the solenoid and allows the latter to be inclined slightly (±3°) by micrometer screws. The resettability of the angles was 1.5′.

The intensity of the magnetic field is measured with an induction coil located in the working region of the solenoid at some distance from the sample. The EMF induced in the coil when the magnetic field changes is led to an electronic integrating circuit, from whose output a voltage proportional to the magnetic field intensity $H_0$ is picked-off. This voltage is impressed on the horizontal deflection plates of both beams of a dual-beam oscilloscope.

A special threshold scanning circuit was employed for the detailed study of the magnetization curves in a given interval of magnetic fields. It starts the beams scanning along the horizontal when some preassigned threshold value of the magnetic field $H_t$, somewhat less than $H_c$, is attained. In this case the deflection is proportional to $H_0 - H_t$, allowing examination on the oscilloscope screen of magnetization curves in the regions of interest with a scale as fine as 100 Oe/cm for a total magnetic field of about 92 kOe.

The magnetization was measured by three induction

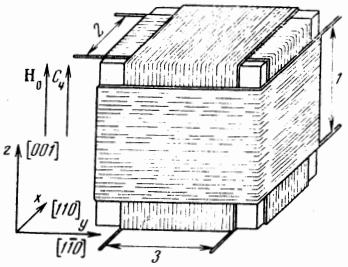


FIG. 1. Arrangement of measuring coils on the sample. 1, 2, 3-leads of coils, axes of which are respectively [001], [110], and [1$\bar{1}$0].

coils wrapped directly on the sample (Fig. 1) and containing 50 turns each of copper wire 20 $\mu$ in diameter. The axis of one of these was parallel to the symmetry axis z⌊001⌋, and the two others were parallel to ⌊110⌋ and ⌊1$\bar{1}$0⌋. The induced EMF that is proportional to $dH_0/dt$ is compensated by a voltage taken from an oppositely connected coil situated far from the sample. The change in the components $M_Z$, $M_y$, and $M_X$ of the sample also gives rise to an EMF in the corresponding measuring coils that is proportional to $(dM_i/dH_0)$ $(dH_0/dt)$ and attains several volts. After integration by simple RC circuits the voltages proportional to the individual magnetization components are fed into the vertical channels of oscilloscopes. The oscillograms of $M_i(H_0 - H_t)$ taken simultaneously from the oscilloscope screen permit establishment of both the magnitude and direction of the sample magnetization vector, which in general does not coincide with the direction of the applied field.

In certain cases the voltages proportional to the magnitudes of two different components of the vector **M** are fed respectively into the vertical and horizontal inputs of an oscilloscope. Such oscillograms (see, for example, Fig. 6) allow a more graphic presentation of the process of growth and rotation of the magnetization vector in a selected plane.

Four samples of $MnF_2$ of different shapes and sizes were investigated. One of these (No. 1) is a cube 0.5 cm on edge. Its edges are oriented along the crystallographic directions [001] (the fourfold symmetry axis), [110], and ⌊1$\bar{1}$0⌋. Three other samples are cylinders with axes parallel to [001]. The diameters and heights of these cylinders are: No. 2—0.8 and 2.5 mm; No. 3—1.5 and 2.9 mm; No. 4—1.85 and 0.2 mm. All samples are nearly perfect monocrystals. No traces of mosaic structure are observed under the polarizing microscope or with x rays. A few small bubbles formed during growth, about 0.1 mm in diameter, are found on one of the edges of No. 1.

## 3. RESULTS

In a magnetic field parallel to the symmetry axis and less than critical, the magnetization is negligibly small. The principal changes in the components of the magnetization vector **M** parallel and perpendicular to the field occur in a narrow interval of magnetic fields near $H_0 \approx 92$ kOe. This portion of the magnetization curves is shown on the dual-beam oscillogram in Fig. 2. The total change of the $M_Z$ components in this interval is calculated to be 98 CGSM. The magnitude of $\Delta M$ serves to determine the scale of the oscillograms along the vertical. The perpendicular components pass

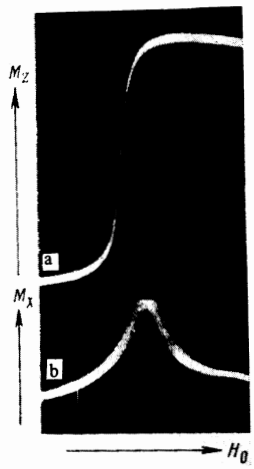


FIG. 2. Oscillograms of longitudinal (a) and transverse (b) components of the magnetization vector as a function of magnetic field intensity in the critical region. As expanded portion of the magnetization curves near $H_0 \approx 92$ kOe is shown.

through a maximum value $M_{\perp 0}$ in the critical interval. For them, calibration is carried out by comparing them with the magnetization change $\Delta M$. Errors associated with non-identity of the measuring channels is eliminated by interchanging them when measuring different components $M_i$. The magnetic field scale was determined by attenuating the deflecting voltage by a calibrated divider and measuring the magnitude of the deflection corresponding to the field of the phase transition. The error in this was 5% or less.

The slope of the $M_Z(H_0)$ curves, which have the meaning of magnetic susceptibility $\chi = dM_Z/dH_0$, increases near $H \approx 92$ kOe, passing through a maximum value $\chi_0$. The calibrations permit expression of the magnitude of $\chi_0$ in absolute units.

The principal results of the investigation of these curves are:

1. The width of the magnetic field interval in which the principal changes in magnetization occur and the associated maximum susceptibility $\chi_0$ depend strongly on the angle $\psi$. Figure 3 shows this dependence for sample No. 1. These curves were taken while changing the orientation of the field in two mutually perpendicular planes. The angle $\psi$ corresponding to the absolute maximum magnetic susceptibility $\chi_0$ is taken as zero.

2. For small $\psi$, and in particular for $\psi = 0$, the magnetic susceptibility differs for different samples and depends, evidently, on their shape (the ratio between the length and width). The values of $\chi_0$ for $\psi = 0$ are: for sample No. 2—0.4 ($\gamma = 3$), for sample No. 3—0.26 ($\gamma = 1.9$), for sample No. 4—0.10 ($\gamma = 0.1$). Figure 4 shows portions of the magnetization curves near $H_C$ for samples No. 2 and No. 4. One slope is almost four times larger than the other.

3. Whenever it is necessary to trace the connection between individual components of **M** for different magnitudes of magnetic field, the voltages proportional to the two components are applied to the vertical and horitzontal inputs of one beam. This eliminates errors due to nonsynchronization of the beams and gives a more graphic representation of the evolution of **M**. If $M_X$ and $M_y$ are handled in this way (cf. Fig. 2), it is possible to determine the direction of the projection of **M** on the basal plane. The family of maximum magnitudes of these projections, with their directions, is in Fig. 5. The oscillograms were taken with $H_0$ away

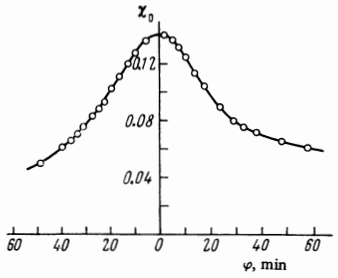


FIG. 3. Angular dependence of the maximum magnitude of the magnetic susceptibility $\chi_0 = dM_Z/dH_0$ in the sublattice flipping region. The angle $\psi$ is between the direction of the applied magnetic field and the crystal symmetry axis.

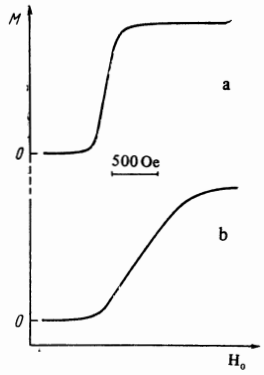


FIG. 4. Portions of the magnetization curves $M_Z(H_0)$ near $H_0 \approx 92$ kOe for two cylindrical samples: a—diameter 0.8 mm and height 2.5 mm ($\chi_0 = 0.42$ CGSM), b—diameter 1.85 mm and height 0.2 mm ($\chi_0 = 0.1$ CGSM).

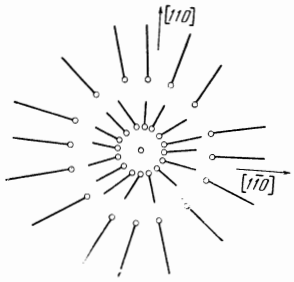


FIG. 5. Family of maximum projections of the sample magnetization vector on the (001) plane during its rotation in an applied magnetic field $H_0 = 92$ kOe of varying orientation ($\psi = 10'$ and $20'$). The displacement of the projections from the origin is proportional to the projection of the applied magnetic field on the (001) plane.

from the symmetry axis by $\psi = 10'$ and $\psi = 20'$ in different azimuths. As is seen from the figure, the orientation of the projection $M_{\perp 0}$ in the basal plane as the vector **M** rotates is dictated mainly by the direction of the projection of the applied field in this plane.

4. For any angle $\psi$ it is always possible to choose an azimuth for which $M_y$ is identically and reproducibly zero for any magnetic field intensity. We can thus get complete information about the behavior of **M** in the xz plane. One of these oscillograms, obtained at $\psi = 40'$, is in Fig. 6a. The arrow indicates the direction of rotation of the sample magnetization vector as the magnetic field is increased. Within the critical field region the magnetic moment of the sample is parallel to the applied field. The trajectory of the rotation vector is nearly a semicircle with a center at $M_\perp = 0$, $M_Z = \Delta M/2$.

5. When $\psi$ is reduced to $30'$ this picture is practically unchanged. With further reduction, the curves come closer to the $M_X$ axis (Fig. 6b), and the maximum projection of the vector **M** on the basal plane decreases sharply (Fig. 7). One can choose a direction for the external field (corresponding to $\psi = 0 \pm 1'$) for which $M_{\perp 0}$ does not exceed 5% of its greatest magnitude.

## 4. DISCUSSION

1. The dependence of magnetic susceptibility on shape (demagnetization factor N) is a general property

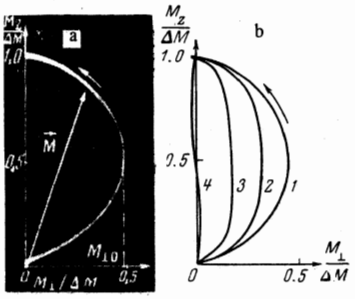


FIG. 6. a–oscillogram showing the growth and rotation of the sample magnetization vector during sublattice flipping near $H_0 \approx 92$ kOe. The arrow indicates direction of rotation as the field increases. Sample No. 1, $\psi = 40'$; b–family of oscillograms taken at various angles: $1-\psi = 40'$; $2-\psi = 17'$; $3-\psi = 7'$; $4-\psi = 0$.

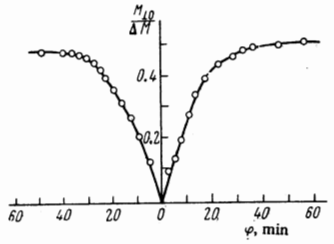


FIG. 7. Angular dependence of the maximum projections of the sample magnetization vector on the (001) plane.

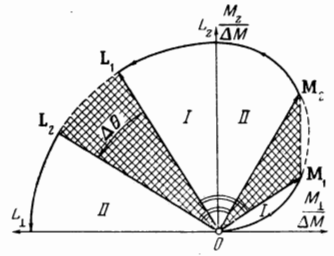


FIG. 8. Diagram showing rotation of the antiferromagnetism vector L (left) and magnetization M (right) during sublattice flippings in an inclined field ($\psi < \psi_c$). The arrows indicate direction of rotation in phases I and II. The dashes delineate the angles belonging to phase instability regions and realized in domain walls.

of domain structures in magnets.[1] If such a dependence were not detected, the absence of domain structure would be inferred. These measurements disclose the conditions under which one can expect domain structure to appear in this crystal.

On the other hand, a dependence of magnetic susceptibility on sample shape appears not only with domain structures but also in other cases when the susceptibility is absolutely large. In fact, the properties of an antiferromagnet are determined by the internal magnetic field in the sample $H_i = H_0 - NM$, which coincides with the external field only in infinitely long cylinders placed in a longitudinal field ($N = 0$). Hence the measured susceptibility $\chi = dM_Z/dH_0$ does not coincide, generally speaking, with the "true" susceptibility $\chi' = dM_Z/dH_i$, but is related to it by

$$(1-c)B_1 + cB_2 = H_0.$$

For large $\chi'$ the measured susceptibility is completely determined by sample shape: $\chi \approx 1/N$. This means, in particular, that in an infinitely thin disk placed perpendicular to a magnetic field, the susceptibility does not exceed $1/4\pi$, even if the magnetization process occurs uniformly over the sample.

If the "true" susceptibility $\chi'$ goes to infinity, i.e., if for some critical value of internal field a first-order magnetic phase transition occurs, a domain structure appears in the sample ($N \neq 0$). The average magnetic susceptibility in this case can be calculated from the principle of magnetic flux conservation.[1] In the case of an infinitely thin plate ($N = 4\pi$) for a concentration c of magnetic phase with induction $B_2 = H_C + 4M_2$, we can write

$$\chi = \chi' / (1 + N\chi').$$

From this condition the average magnetization of the sample can be expressed in terms of the magnetization of the individual phases, and the average susceptibility of the sample turns out to be equal to $1/4\pi$.

Comparing these conclusions with experimental results, it must first be realized that quantitative agreement can be obtained only for samples of ellipsoidal shape. For convenience, we used cylinders in our experiments, for which the demagnetizing fields are nonuniform, so that a definite factor N cannot be ascribed to them. The concept of effective shape factor, which is usually used for cylindrical ferromagnetic samples, is inapplicable in this case. Inhomogeneity of the demagnetizing fields leads to a broadening of the region of magnetic fields in which an increase in magnetization is observed and to a lowering of the measured susceptibility. In spite of this, the experiment shows that for a range of several hundred Oersteds about $H_0 \approx 92$ kOe and a narrow range of $\psi$ of the order of several tens of minutes, the measured susceptibility exceeds $1/4\pi$ and depends on the sample shape. The susceptibility of the cylinder ($\gamma = 3.0$) is almost four times greater than the susceptibility of the flat sample ($\chi_0 = 1.3/4\pi$ for $\gamma = 0.1$), and the latter is close to the expected value for an infinitely thin disc.

The results are therefore completely consonant with the idea that domain structure exists in these samples in the ranges of $H_0$ and $\psi$ indicated above.

2. The study of the process of increase and rotation of the magnetization vector of $MnF_2$ in critical field is of interest from the following points of view. The theoretical model of sublattice flipping of a uniaxial antiferromagnet[7,8] establishes a definite connection between the modulus of the vector **M** and its direction $\theta$ in the crystal, and this has not been confirmed experimentally. Already, the known properties of $MnF_2$ are in extremely good agreement with even the simplest theoretical calculations. Hence this crystal is a good choice for comparing the theoretical dependence of M on $\theta$ with the experimental one.

On the other hand, regardless of the degree of agreement with theory, a determination of the equilibrium curve $M(\theta)$ is of interest in that possible deviations from it yield unequivocal information about magnetic stratification phenomena in the crystal.

In the accepted theoretical model[5-8] this crystal is considered to be a two-sublattice antiferromagnet. The magnetizations of both sublattices $\mathbf{M}_{01}$ and $\mathbf{M}_{02}$ are equal in size but opposite in direction. There is no spontaneous magnetization: $\mathbf{M} = \mathbf{M}_{01} + \mathbf{M}_{02} = 0$, and the antiferromagnetism vector $\mathbf{L} = \mathbf{M}_{01} - \mathbf{M}_{02}$ is directed along the fourfold symmetry axis. A deviation of the vector **L** from the equilibrium position by angle $\theta$ leads to an increase of anisotropy energy: $E_A = k_0 \sin^2\theta$. According to the model an external mag-

netic field $\mathbf{H}_0$ does not change the magnetization of the individual sublattices but can affect their relative orientation. Hence the magnetization vector $\mathbf{M}$ is always perpendicular to the antiferromagnetism vector $\mathbf{L}$: $\mathbf{M} \cdot \mathbf{L} = 0$.

In an external field $\mathbf{H}_0$ of a certain magnitude directed parallel to the symmetry axis z, the vector $\mathbf{L}$ rotates by an angle $\pi/2$ in a plane perpendicular to the field (Fig. 8, left). The loss of anisotropy energy is compensated by a gain in magnetic energy:

$$E_M = -1/2 \mathbf{M}\mathbf{H}_c = -1/2 MH_c \sin\theta.$$

This equality yields a simple relation between the modulus of the magnetization vector and its equilibrium angle of rotation $\theta$: $M = 2k_0 H_C^{-1} \sin\theta$. This relation is indicated by the semicircle in Fig. 8 (right). In this approximation, only the principal interactions that determine the form of $M(\theta)$ are taken into account. A more rigorous approach[8,9] requires consideration of other, finer interactions and, especially, the finite temperature. However, the rather good qualitative agreement of the experimental curve taken at $\psi = 40'$ (Fig. 6a) with the approximate calculation shows that these factors do not alter the general picture much. Hence, we may assume that rotation of the vector $\mathbf{L}$ occurs in the same plane with the vectors $\mathbf{H}_0$ and $\mathbf{M}$, and the process of sublattice rotation can be reproduced (see Fig. 8) from the experimental observed function $M(\theta)$.

It is important to note that the form of the $M(\theta)$ curve for a uniform sublattice rotation (for $\psi \ll 1$) should not depend on the angle $\psi$. This is confirmed by experiment in the region of angles from $60'$ to $30'$, where the theory predicts a uniform rotation of the sublattices without phase transitions.

3. We shall be interested not so much in the reasons for the appearance of a specific dependence of $\mathbf{M}$ on $\theta$ and its relation to rotation of $\mathbf{L}$ as in finding the actual curve that belongs to stable states with a given vector $\mathbf{M}$. If the crystal is divided up into spatial regions, the specific magnetization $\mathbf{M}_i$ of each region should correspond to one of the points of the equilibrium $M(\theta)$ curve. But the total magnetization of the sample belongs to this curve only if its magnetization is uniform.

The experimental curves in Fig. 6b show that the total magnetization vector of the sample, in the process of rotation with $\psi < 30'$, runs through a number of values that belong to states of absolute instability. This means that the total magnetization does not coincide with the local magnetization. Thus, we are forced to conclude that in the region of angles $\psi < 30'$ and in a critical interval of magnetic fields, the crystal is divided up into regions the specific magnetizations of which differ and correspond to different points of the thermodynamic equilibrium $M(\theta)$ curve.

4. Let us consider the mechanism of such stratification under the conditions of a first-order magnetic transition. If the angle $\psi$ does not exceed the critical magnitude $\psi_C$, the process of rotation of the vector $\mathbf{L}$ is not continuous and occurs in the following way (see Fig. 8). As the external magnetic field is increased and especially as it approaches its critical value $H_C$ the vector $\mathbf{L}$ of the initial phase deviates from the symmetry axis z by an angle $\theta_{1C}$. The magnitude of this angle that determines the stability limit of the first phase depends on the orientation of the external field and varies from $\theta_{1C} = 0$ at $\psi = 0$ to $\theta_{1C} = \pi/4$ for $\psi = \psi_C$. With further increase of field, a first-order phase transition occurs in an infinitely long cylinder ($N = 0$).[7,8] The direction of the $\mathbf{L}$ of the second phase also depends on the angle $\psi$. In the phase transition the vector $\mathbf{L}$ completes an abrupt rotation by an angle $\Delta\theta = \theta_{2C} - \theta_{1C}$. The vector $\mathbf{M}$ also changes its orientation abruptly by an angle $\Delta\theta$ and simultaneously changes in absolute magnitude. The portion of the $M(\theta)$ curve shown in Fig. 8 by dashes corresponds to unstable states and is not realized in practice.

According to domain theory,[1,4,9] magnetic phases I and II coexist in samples with nonzero demagnetization factor over a finite interval of magnetic fields and form periodic alternating regions. As the field is increased, the volume occupied by phase II increases by movement of the domain walls. Instead of an abrupt change in the total magnetization of the sample, one observes that it steadily increases along the trajectory of $\mathbf{M}$ shown by the vertical dashed line in Fig. 8.

When the sublattices flip, a transverse component of the magnetization appears that is characteristic of the magnetization of the coexisting phases. As $\psi$ is reduced to zero, so do the magnitudes of $M_{\perp 1}$ and $M_{\perp 2}$.

In the domain structure the phases are divided by domain walls in which the vectors $\mathbf{L}$ and $\mathbf{M}$ undergo a smooth rotation by $\Delta\theta$. In particular, when $\psi = 0$ there is a 90-degree domain wall. As $\psi$ increases, the angle of rotation $\Delta\theta$ in the wall decreases, going to zero when $\psi = \psi_C$. When $\psi > \psi_C$ the domain structure disappears and the sublattice rotation process becomes uniform over the sample volume. The domain walls have their own magnetization, but their contribution to the total sample magnetization is small in the same degree as the volume occupied by them is small.

5. The mechanism described here may not be the only one for a given crystal. It is known that the character of the domain structure is quite sensitive to defects in the sample. However, comparison of the theoretical $M(\theta)$ curves with the experimental ones shows up a series of extremely important coincidences. The change in magnetization during sublattice flipping occurs first along a curve that is close to the thermodynamically stable one. Departure from this curve is characterized by a preferential growth of the longitudinal component of $\mathbf{M}$ while $M_\perp$ remains practically unchanged. The vertical portion of the $M(\theta)$ curve also obviously corresponds to a region where domain structure exists. The insufficiently sharp transition from the equilibrium trajectory of $M(\theta)$ to the vertical portion can be understood by taking into account the inhomogeneity of the demagnetizing fields in the sample, the shape of which (cube) differs significantly from ellipsoidal. In accordance with theory the maximum magnitude of the transverse component of magnetization falls sharply (Fig. 7) with decreasing angle $\psi$. Interestingly, the interval of angles in which signs of magnetic stratification are observed ($\psi_C \approx 30'$) is close to the calculated region of existence of a phase transition of the first kind in this antiferromagnet. Finally, the magnitudes of the susceptibilities of the samples are close to those expected for domain structure formation.

By juxtaposing the experimental (Fig. 6) and theoretical (Fig. 8) $M(\theta)$ curves, one can find the magnitudes and directions of the magnetization vectors $M_1$ and $M_2$ of the individual phases and the rotation angles of M and L in the domain walls for different orientations of the applied magnetic field. Since the magnetizations of continuous phases in this case differ not only in direction but also in absolute magnitude, the domain structure of $MnF_2$ in the critical field region differs from that of a ferromagnet and is analogous to the structure of the intermediate state of a superconductor.

We are presently refining and analyzing other experimental data that reflect the features of domain wall motion under the conditions of this type of magnetic stratification. The results will be published soon.

We consider it our pleasant duty to express our gratitude to I. A. Privorotskiĭ for fruitful discussions, L. M. Semenko for considerable help with the experiment, V. G. Bar'yakhtar and A. E. Borovik for numerous discussions and constant interest, and B. I. Verkin for supporting the research.

[1]L. D. Landau and E. M. Lifshitz, Élektrodinamika sred (Electrodynamics of Continuous Media), Fizmatgiz, 1959.

[2]S. V. Vonsovskiĭ and Ya. S. Shur, Ferromagnetizm (Ferromagnetism), Gostekhizdat, 1948.

[3]J. H. Condon, Phys. Rev. **145**, 526 (1966).

[4]I. A. Privorotskiĭ, Zh. Eksp. Teor. Fiz. **52**, 1755 (1967); **56**, 2129 (1969) [Sov. Phys.-JETP **25**, 1167 (1967); **29**, 1145 (1969)].

[5]L. Néel, Ann. Phys. **5**, 232 (1936).

[6]E. A. Turov, Fizicheskie svoistva magnitouporyadochennykh kristallov (Physical Properties of Magnetically Ordered Crystals), Izd. Akad. Nauk SSSR, 1963.

[7]M. I. Kaganov and G. K. Chepurnykh, Fiz. Tverd. Tela **11**, 911 (1969) [Sov. Phys.-Solid State **11**, 745 (1969)].

[8]V. A. Popov and V. I. Skidonenko, Fizika kondensirovannogo sostoyaniya (Physics of the Condensed State), Tr. FTINT, No. 7, Kharkov, 1970, p. 49.

[9]V. G. Bar'yakhtar, A. E. Borovik, and V. A. Popov, ZhETF Pis. Red. **9**, 634 (1969) [JETP Lett. **9**, 391 (1969)].

[10]A. J. Mitsek, P. F. Gaidanskij, and V. N. Pushkar, Phys. Stat. Sol. **38**, 69 (1970).

[11]J. S. Jacobs, J. Appl. Phys. **32**, 61S (1961).

[12]H. Rohrer and H. Thomas, J. Appl. Phys. **40**, 1025 (1969).

Translated by L. M. Matarrese
69